IMPROVEMENT OF WEB SPACING CHARACTERISTICS BY TWO TYPES OF GUIDE ROLLERS

by

H. Hashimoto
Tokai University
JAPAN

ABSTRACT

In the manufacturing fields of plastic sheet, paper, magnetic tape, thin metal plate, photographic film etc., the web transporting systems supported by guide rollers are often used. In such systems, it is of cardinal importance to control the web spacing between the traveling web and guide rollers. For example, when the guide roller is used as turn bar in the commercial web offset press or used as dryer in the coating processes of web, it is sometimes needed to keep sufficient air film thickness between web and roller for avoiding the web defects due to surface roughness, stain and lack of uniforming . On the other hand, when the guide roller is used as drag roller, it is desirable to remove the entrained air between web and roller for keeping enough level of traction.

In this paper, two types of guide rollers are presented to improve the web spacing characteristics, one of which is hybrid type hollow porous roller for keeping the sufficient web spacing, and the other is grooved type roller for removing the entrained air. In the hybrid type hollow porous roller, the pressurized air is added to the lubrication air flow between web and roller from inside the roller. Then, the web spacing characteristics are improved by the hybrid effects of hydrodynamic pressure due to web movements and hydrostatic pressure due to pressurized added air through the roller. The relations between web spacing and web traveling velocity are measured under various supply pressures. Moreover, the relations between web spacing and web tension are examined. The contactless optical sensor, which can measure the variation of the quantities of reflected light from the back surface of web according to the variation of web spacing, is used to obtain the web spacing under various conditions. In the grooved rollers, the method for the estimation of web spacing by using the concept of equivalent spacing between web and roller is presented, and the web spacing is measured by the same experimental apparatus used in the case of hollow porous roller. From the calculated and measured results obtained, the effectiveness of two types of guide rollers on the web spacing is clarified.

NOMENCLATURE

b = groove pitch (m)
b_g = groove width (m)
$2B$ = wrap angle of web (deg)
E = elasticity modulus of web (Pa)
h = web spacing (m)
h_{eq} = equivalent web spacing (m)
h_g = groove depth (m)
k = permeability of porous roller (m^2)
L = web width (m)
n = number of groove
p = film pressure (Pa)
p_a = ambient pressure (Pa)
p_s = supply pressure (Pa)
q = volume rate of air flow (m^3/s)
R = roller radius (m)
s_g = cross sectional area of a groove (m^2)
t = thickness of hollow porous roller (m)
t_f = thickness of web (m)
T = tension per unit width of web (N/m)
u = web deflection (m)
U = traveling velocity of web (m/s)
x = coordinate in the moving direction (m)
z = coordinate in the axial direction (m)
μ = air film viscosity (Pa·s)
ν = Poisson's ratio of web

INTRODUCTION

In the manufacturing fields of plastic, paper, magnetic tape, thin metal plate, photographic film etc., the web transporting systems supported by guide rollers as shown in Fig.1 are often used. In such guide roller systems, the traveling web brings the surrounding air into the gap between web and guide roller, and then the web is lifted slightly by the film pressure generated due to the entrained air viscous effect (1). Therefore, it is of cardinal importance to control the web spacing suitably according to the objective of guide roller systems. For example, when the guide roller is used as turn bar in the commercial web offset press or used as dryers in the coating process of web as shown in Fig.2, it is sometimes needed to keep more sufficient web spacing for avoiding the web defects due to surface roughness, stain and lack of uniforming. On the other hand, when the guide roller is used as drag roller, it is desirable to remove the entrained air between web and roller for keeping enough level of traction.

For the former purposes, it may be effective to utilize the hybrid type foil bearings as guide rollers for supporting the traveling web (2). In this type of rollers, it is expected to control hydrostatic effect (externally pressurized effect). Wildmann and Wright (3) originally analyzed the infinitely long hybrid foil bearings and they concluded that the effect of even small external pressurization in a self-acting foil bearing is very important. Barlow and Wildmann (4) and Baumann (5) investigated the axisymmetric, externally pressurized porous foil bearings, in which flow is only across the foil or along the axis of the supporting spindle. Yabe et al. analyzed the hybrid performance of infinitely long, porous foil bearings neglecting the axial flow in the bearing gap for three cases with no relative foil velocity (6), with a small relative foil velocity (7) and with a large relative foil velocity (8), respectively. Moreover, Hashimoto (9) analyzed the finite width, hybrid

porous foil bearings considering the axial flow in the bearing gap. However, the experimental study on the finite width porous foil bearing has not been presented.

For removing the entrained air between web and guide roller, it has been often used the grooved roller experimentally, but, as far as the author knows, no published paper investigating the effects of grooved rollers from a view point of web handling system design can be seen in the literatures.

In this paper, the idea of two types of guide rollers are presented to improve the web spacing, one of which is hybrid type hollow porous roller as shown in Fig.3(a) for keeping the sufficient web spacing and the other is circumferentially grooved type roller as shown in Fig.3(b) for removing the entrained air.

THEORETICAL ANALYSIS OF WEB SPACING

Web Spacing Analysis for Flat Roller

Before analyzing the web spacing for two types of rollers, let us introduce the outline of web spacing analysis for ordinary flat type roller. The foil bearing model, as shown in Fig.4, is generally applied to analyze the web spacing in the web wrapped region (Region II), in which the film pressure and web spacing are obtained theoretically by solving the following Reynolds equation and web elastic equation simultaneously.

$$\frac{\partial}{\partial x}\left(h^3\frac{\partial p}{\partial x}\right)+\frac{\partial}{\partial z}\left(h^3\frac{\partial p}{\partial z}\right)=6\mu U\frac{\partial h}{\partial x} \quad \text{(for incompressible fluid)} \quad [1.a]$$

$$\frac{\partial}{\partial x}\left(h^3 p\frac{\partial p}{\partial x}\right)+\frac{\partial}{\partial z}\left(h^3 p\frac{\partial p}{\partial z}\right)=6\mu U\frac{\partial (ph)}{\partial x} \quad \text{(for compressible fluid)} \quad [1.b]$$

$$\frac{Et_f^{\,3}}{12\left(1-\nu^2\right)}\nabla^2\nabla^2 h+\frac{T}{R}\left(1-R\frac{\partial^2 h}{\partial x^2}\right)=p-p_a \quad [2]$$

Assuming that the web is perfectly flexible and the web deflection in the axial direction is small as compared with the deflection in the traveling direction, the web elastic equation [2] is simplified as follows:

$$\frac{T}{R}\left(1-R\frac{\partial^2 h}{\partial x^2}\right)=\frac{1}{L}\int_0^L (p-p_a)dz \quad [3]$$

In Regions I and III, the pressure is equal to the ambient pressure, then it is expressed as:

$$p=p_a \quad [4]$$

The web deflection in Regions I and III is determined from the following equation.

$$\frac{d^2 u_{\mathrm{I,III}}}{dx^2}=0 \quad [5]$$

Moreover, the relation between the web spacing and the web deflection in Region II is given as follows:

$$u_{II} = h + \sqrt{R^2 - x^2} \qquad [6]$$

Solving Eqs.[1], [3], [4], [5] and [6] simultaneously, as has already been done in Reference (1), with the suitable boundary conditions and continuity conditions between Regions I and II and Regions II and III, and applying the curve fitting technique to the numerical solutions, the formula for the web spacing for the flat roller is derived as follows:

$$h = R\left(\frac{6\mu U}{T}\right)^{\frac{2}{3}}\left(0.643 - \frac{1.185}{\lambda} + \frac{0.948}{\lambda^2}\right) \qquad \text{(for incompressible fluid)} \qquad [7.a]$$

$$h = R\left(\frac{6\mu U}{T}\right)^{\frac{2}{3}}\left(0.589 - \frac{1.614}{\lambda} + \frac{1.764}{\lambda^2}\right) \qquad \text{(for compressible fluid)} \qquad [7.b]$$

where:

$$\lambda = \frac{L}{2R}\left(\frac{6\mu U}{T}\right)^{-\frac{1}{3}} \qquad \text{(valid for } \lambda > 0.2\text{)} \qquad [7.c]$$

Web Spacing Analysis for Hollow Porous Type Roller

Comparing with the flat roller as described above, a new type of hollow porous roller as shown in Fig.5 has an advantage to control the web spacing suitably according to the variation of operation conditions in the web handling systems. The guide roller system consists of the web and hollow porous type roller. Pressurized air is added from inside the hollow porous roller to the hydrodynamic air flow in the web spacing. Then, the web spacing characteristics are improved by the hybrid effects of hydrodynamic pressure due to web movements and hydrostatic pressure due to pressurized added flow through the hollow porous roller.

The geometrical relation between hollow porous type roller and web is schematically illustrated in Fig.6. In the analysis of web spacing, the following assumptions are made:

(a) The web is perfectly flexible and the bending stiffness of web can be neglected.

(b) The web tension is constant.

(c) The porous material is isotropic and the flow within the porous roller can be treated as the flow in the capillary.

(d) The surface of porous roller is sufficiently smooth, so the surface roughness of roller can be neglected.

Under these assumptions, the modified Reynolds equation governing the film pressure developed in the web spacing is given as follows:

$$\frac{\partial}{\partial x}\left(h^3\frac{\partial p}{\partial x}\right) + \frac{\partial}{\partial z}\left(h^3\frac{\partial p}{\partial z}\right) + \frac{12k}{t}(p_s - p) = 6\mu U\frac{\partial h}{\partial x} \qquad [8.a]$$

(for incompressible fluid)

$$\frac{\partial}{\partial x}\left(h^3 p\frac{\partial p}{\partial x}\right) + \frac{\partial}{\partial z}\left(h^3 p\frac{\partial p}{\partial z}\right) + \frac{12k}{t}p(p_s - p) = 6\mu U\frac{\partial (ph)}{\partial x} \qquad [8.b]$$

(for compressible fluid)

Solving numerically a set of simultaneous equations [3], [4], [5], [6] and [8] with the suitable boundary and continuity conditions, the numerical solutions of web spacing will

be determined for prescribed parameters.

Web Spacing Analysis for Circumferentially Grooved Roller

In order to take the effects of circumferential grooves into consideration in the web spacing analysis, a concept of equivalent web spacing h_{eq} as shown in Fig.7 is introduced.

In Region II (web wrapped region) in Fig.4, the shear flow (Couette type flow) is predominant, then the volume rate of air flow in the moving direction is approximately expressed as follows:

$$q \cong \frac{U}{2}\left(hL + ns_g\right) = \frac{U}{2}h_{eq}L \qquad [9]$$

where:

$$s_g = \begin{cases} \frac{1}{2}h_g b_g & \text{(for triangular groove)} \\ h_g b_g & \text{(for rectangular groove)} \end{cases} \qquad [10]$$

and the equivalent spacing h_{eq} is given from Eq.[7] as follows:

$$h_{eq} = R\left(\frac{6\mu U}{T}\right)^{\frac{2}{3}}\left(0.643 - \frac{1.185}{\lambda} + \frac{0.948}{\lambda^2}\right) \quad \text{(for incompressible fluid)} \qquad [11.a]$$

$$h_{eq} = R\left(\frac{6\mu U}{T}\right)^{\frac{2}{3}}\left(0.589 - \frac{1.614}{\lambda} + \frac{1.764}{\lambda^2}\right) \quad \text{(for compressible fluid)} \qquad [11.b]$$

Evaluating the web spacing h from Eq.[9]:

$$h = h_{eq} - \frac{ns_g}{L} \qquad [12]$$

Equation [12] shows the modification of the web spacing with groove to the web spacing without groove.

WEB SPACING MEASUREMENTS

To confirm the effectiveness of two types of guide rollers, the web spacing is measured for flat, hollow porous type and circumferentially grooved rollers.

Figure 8 shows the outline of experimental apparatus for measuring the web spacing. The audio-tape is used as the web, which is driven by the capstan motor pressed with nipped roller ④ and sent from the unwinding reel ① to the winding reel ②. The web traveling velocity is controlled by the capstan motor ③ to maintain the constant velocity, and the velocity is equal to the surface velocity of the shaft of capstan motor, which is calculated from the rotational speed of motor (rpm) measured by the tachometer. The web tension is generated by the lever with the spring ⑤. The wrap angle of web can be set by selecting the position of guides as $2B$=66 (deg), 110 (deg) and 140 (deg), in which each guide is supported by the ball bearing with very low friction. The surface roughness height of roller and web used in the experiments was measured by the surface roughness measuring instrument. The maximum surface roughness height of roller was within 2 (μm) and the roughness height of web was negligible as compared with the roughness

height of roller. In the case of hollow porous roller, the compressed air was supplied to the inside hollow porous roller through air tube from the compressor. The viscosity of the air was 1.822×10^{-5} (Pa·s) at the atmospheric temperature. The web spacing was measured by the contactless optical sensor ⑥ set just under the roller. In this type of optical sensor, the variation of the quantity of reflected light from the back surface of the web can be measured according to the variation of web spacing and the data obtained is converted to the variation of output voltage. The resolution of the sensor is 0.5 (μm). The overview of experimental apparatus is shown in Fig.9.

The web spacing was measured for the combinations of several fixed parameters such as web traveling velocity U, air supply pressure p_s, web wrap angle $2B$, groove depth h_g, groove width b_g and web tension T. Ten data points were obtained for each fixed parameter.

RESULTS AND DISCUSSIONS

A comparison of the calculated web spacing and the measured spacing is shown in Figs.10 through 17, in which the maximum and minimum values of measured data for each fixed parameter are indicated by the error bars.

Figures 10 and 11 show the results for the flat roller. The dimensions of flat roller used in the measurements are shown in Table 1.

Figure 10 shows the relation between the web spacing and the web traveling velocity for the web tension of T=70 (N/m) and web wrap angle of $2B$=66 (deg), in which the experimental results are compared with the calculated results. In both results, the web spacing increases with an increase of web traveling velocity and the experimental results agree with the calculated results within an acceptable accuracy.

The variation of web spacing with web tension is shown in Fig.11 for $2B$=66 (deg). The web spacing decreases with an increase of web tension, and the web spacing becomes larger as the web traveling velocity increases for the same web tension. As can be seen in the figure, the calculated results agree with the measured results within an acceptable accuracy.

The calculated and measured results of web spacing for the hollow porous type roller are shown in Figs.12 through 14. The dimensions of hollow porous roller used in the measurements are shown in Table 2.

Figure 12 shows the variations of web spacing with air supply pressure for various values of web traveling velocity in the case of web tension of T=70 (N/m) and web wrap angle of $2B$=66 (deg). For the web traveling velocity of U=0, the hydrostatic effect due to the pressurized air flow supplied through the hollow porous roller is dominant in the lubrication air flow between the web and roller, and then the web spacing increases with increasing in the air supply pressure. When the web is driven with the capstan motor, the hydrodynamic pressure due to the web movement is added to the hydrostatic effect, and then the web spacing increases with increasing in the web traveling velocity for a fixed supply pressure. However, the rate of an increase is not constant for a given supply pressure, and it strongly depends on the magnitude of supply pressure. The numerical results agree well with the measured results.

Figure 13 shows the variation of web spacing with web traveling velocity for various values of supply pressure, in which the measured data points for the flat roller, which are indicated by the white plots, are compared with the calculated results. As can be seen in the figure, the web spacing for the flat roller increases continuously with increasing in the web traveling velocity and the calculated results agree well with the experimental data. The magnitude of web spacing is less than 10 (μm) for a wide range of web traveling velocity up to U=12 (m/s). However, the web spacing for the hollow porous roller is much lager than that for the flat roller. For the fixed value of air supply pressure, the web

spacing increases continuously for a range of relatively small web traveling velocity and it takes maximum value at the certain value of traveling velocity. Then, the web spacing decreases with increasing in the velocity. In the case of the supply pressure of p_s=0.1 (MPa), the web spacing reaches to zero value at the web traveling velocity of U=12 (m/s), and then the web is in contact with the roller surface. For a large velocity, the hydrodynamic pressure becomes relatively large as compared with the hydrostatic pressure, so the inverse air flow from the web spacing to the inside of porous roller will be induced and the web spacing may be decreased as shown in the figure. It follows from this figure that the web spacing can be controlled actively with suitable choice of the combined values of web traveling velocity and air supply pressure, and then it is possible to keep suitable spacing for avoiding the surface damage of web due to friction between web surface and roller surface. The calculated results for hollow porous roller also agree with the experimental results.

Figure 14 shows the variation of web spacing with web tension for the web traveling velocity of U=6.2 (m/s) and the web wrap angle of $2B$=66 (deg). As can be seen in the figure, the web spacing decreases continuously with increasing in the web tension and the rate of a decrease in the hollow porous roller becomes larger than the rate in the flat roller.

The calculated and measured results of web spacing for the grooved roller are shown in Figs.15 through 17. The triangular and rectangular grooved rollers are examined. The dimensions of these two types of grooved rollers are shown, respectively, in Table 3 and Table 4.

Figure 15 shows the variation of web spacing with web traveling velocity for the rectangular grooved roller. The web wrap angle and web tension are, respectively, fixed at $2B$=66 (deg) and T=70 (N/m). As can be seen in the figure, the web spacing for the grooved roller becomes much smaller than the spacing for the flat roller, because an amount of entrained air escapes through the circumferential grooves and then the hydrodynamic film pressure generated in the web spacing decreases considerably. The calculated results agree with the measured results within an acceptable accuracy.

Figure 16 shows the variation of web spacing with web traveling velocity for the triangular grooved roller. As the cross sectional area of groove is the same as the area of rectangular groove, the same tendency is observed as the case of rectangular grooved roller. The fairly good agreement is seen between the calculated results and the measured results.

Figure 17 shows the variation of web spacing with web tension for the triangular grooved roller. The web spacing decreases with an increase of web tension and the web spacing for the triangular grooved roller becomes much smaller than the spacing for the flat roller. From these calculated and measured results, it is confirmed the effectiveness of groove on the web spacing characteristics.

As presented above, the web spacing can be controlled successfully by using the suitable guide rollers.

By the way, in the web handling systems, the web spacing strongly affect the traveling web behavior such as wrinkling and lateral motion because the traction between web and guide roller is a function of web spacing (10). In the subsequent papers, the present method for the estimation of web spacing will be applied to the wrinkling and lateral motion analyses of traveling web supported by several types of guide rollers treated in this paper.

CONCLUSIONS

The idea of using hollow porous type roller and circumferentially grooved roller was introduced to improve the web spacing characteristics according to the objective of guide roller systems in the web handling processes. The calculated web spacing was compared

with the measured spacing for these two types of guide rollers. The conclusions are as follows:

1. The web spacing can be controlled actively with suitable choice of guide rollers.
2. In the case of hollow porous roller, the web spacing increases in the web traveling velocity and the rate of an increase strongly depends on the magnitude of supply pressure. Moreover, the web spacing decreases continuously with increasing in the web tension and the rate of a decrease becomes larger with increasing in supply pressure.
3. In the case of circumferentially grooved roller, the web spacing decreases considerably as compared with the flat roller by the suitable design of groove geometry.

REFERENCES

1. Hashimoto, H., "Estimation of Air Film Thickness Between Moving Webs and Guide Rollers," Proceedings of the Fourth International Conference on Web Handling, 1997, pp.177-188.

2. Hashimoto, H., "Theoretical Analysis of Externally Pressurized Porous Foil Bearings — Part I: In the Case of Smooth Surface Porous Shaft," Trans. ASME Journal of Tribology, Vol.117, No.1, 1995, pp.103-111.

3. Wildmann, M. and Wright, A., "The Effect of External Pressurization on Self-Acting Foil Bearings," Trans. ASME Journal of Basic Engineering, Vol.87, 1965, pp.631-640.

4. Barlow, E.J. and Wildmann, M., "The Axisymmetric, Perfectly Flexible Foil Bearings with Porous Inlet Restrictor," Trans. ASME Journal of Lubrication Technology, Vol.90, No.1, 1968, pp.145-152

5. Baumann, G.W., "Analysis of a Porous Gas Foil Bearing," Trans. ASME Journal of Lubrication Technology, Vol.93, No.3, 1971, pp.456-464.

6. Yabe, H., Mori, H., Nakayama, S. and Tone, M., "A Study on Externally Pressurized Gas-Lubricated Foil Bearing with Porous Shaft (1st Report) — Bearing Performance with No Relative Foil Velocity," Journal of JSLE, Vol.24, No.3, 1979, pp.154-159 (in Japanese).

7. Yabe, H., Mori, H., Nakayama, S. and Tone, M., "A Study on Externally Pressurized Gas-Lubricated Foil Bearing with Porous Shaft (2nd Report) — Hybrid Bearing Performance with a Small Foil Velocity," Journal of JSLE, Vol.24, No.3, 1979, pp.160-165 (in Japanese).

8. Yabe, H., Mori, H. and Tone, M., "A Study on Externally Pressurized Gas-Lubricated Foil Bearing with Porous Shaft (3rd Report) — Hybrid Bearing Performance with Predominant Hydrodynamic Effect," Journal of JSLE, Vol.25, No.1, 1980, pp.47-54 (in Japanese).

9. Hahimoto,H., "Effect of Foil Bending Rigidity on Spacing Height Characteristics of Hydrostatic Porous Foil Bearings for Web Handling Processes," Trans. ASME Journal of Tribology, Vol.119, No.3, 1997, pp.422-427.

10. Good, J.K., "Shear in Multispan Web Systems," Proceedings of the Fourth International Conference on Web Handling, 1997, pp.264-285.

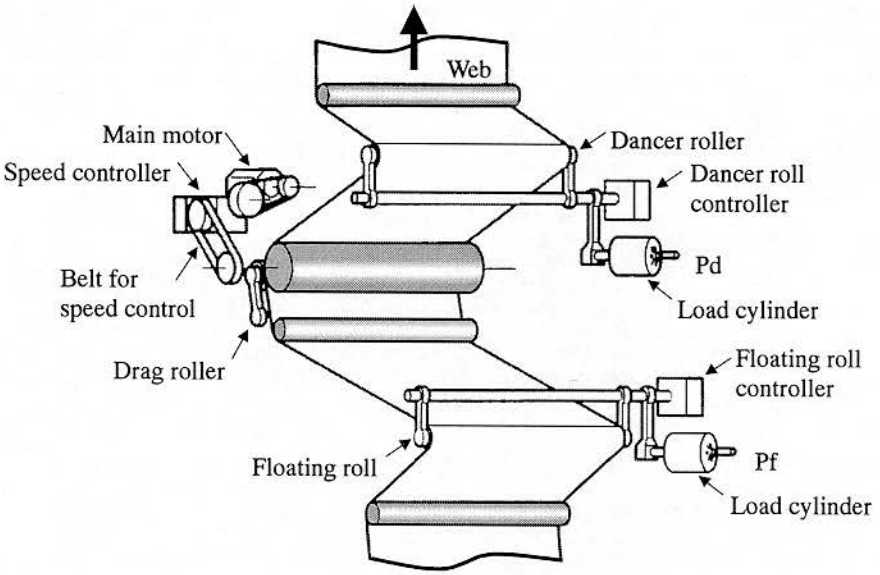

Fig.1 Example of drag roller

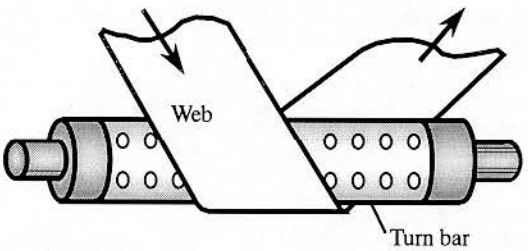

(a) Web path at the folder

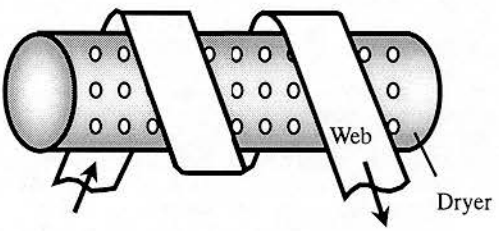

(b) Web drying process

Fig.2 Examples of hydrostatic type guide roller

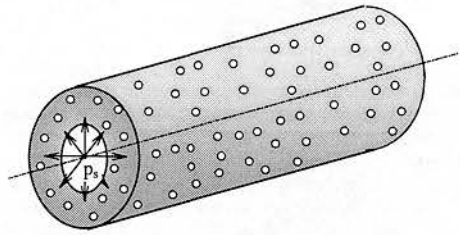

(a) Hollow porous type roller

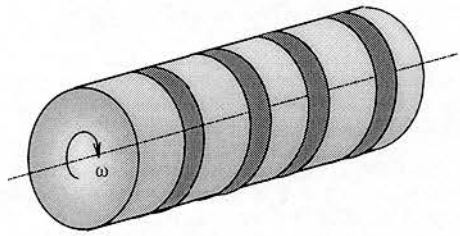

(b) Circumferentially grooved roller

Fig.3 Two types of rollers for improving web spacing characteristics

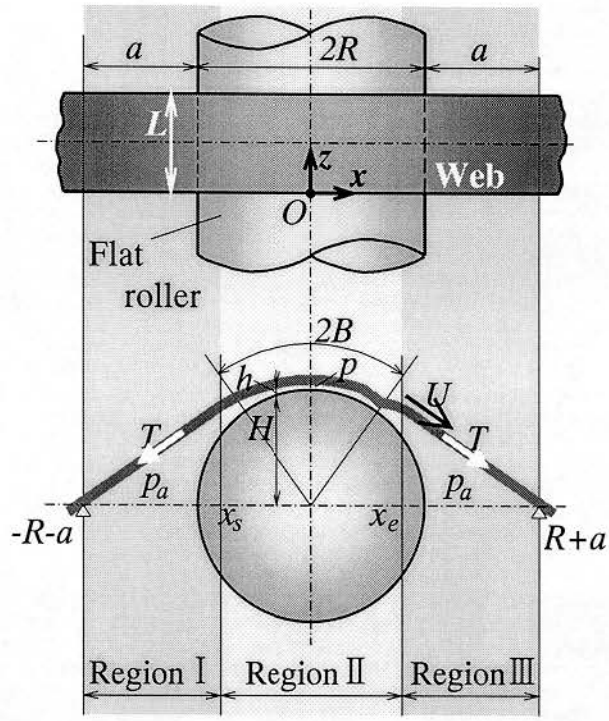

Fig.4 Foil bearing model for flat roller

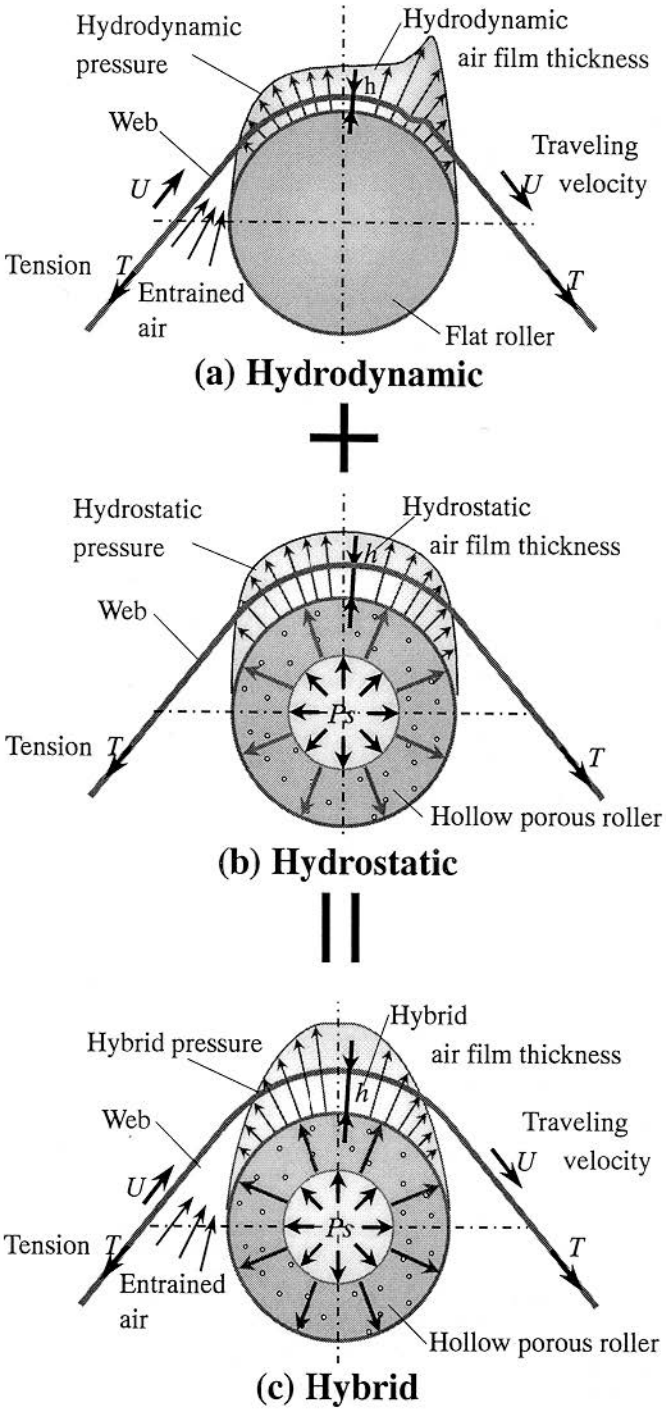

Fig.5 Principle of hollow porous roller

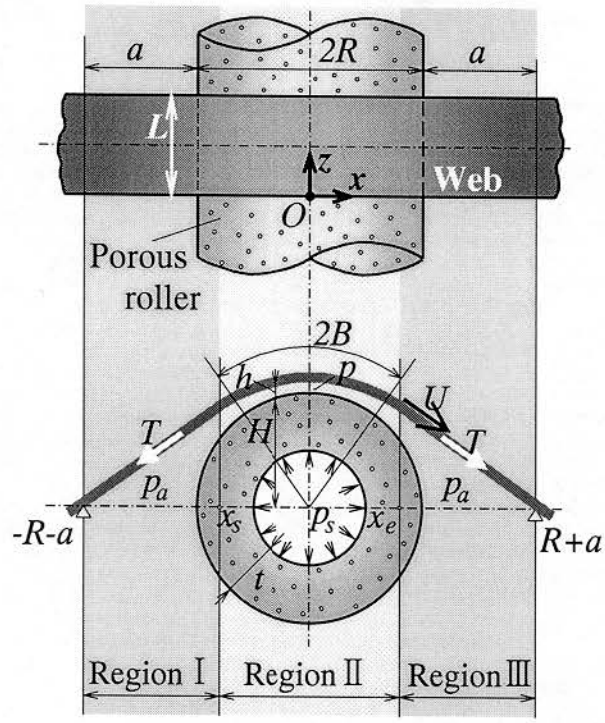

Fig.6 Foil bearing model for hollow porous roller

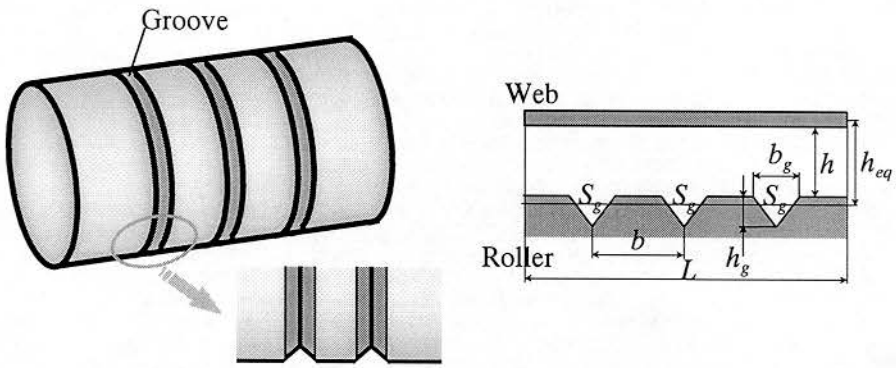

Fig.7 Concept of equivalent web spacing for circumferentially grooved roller

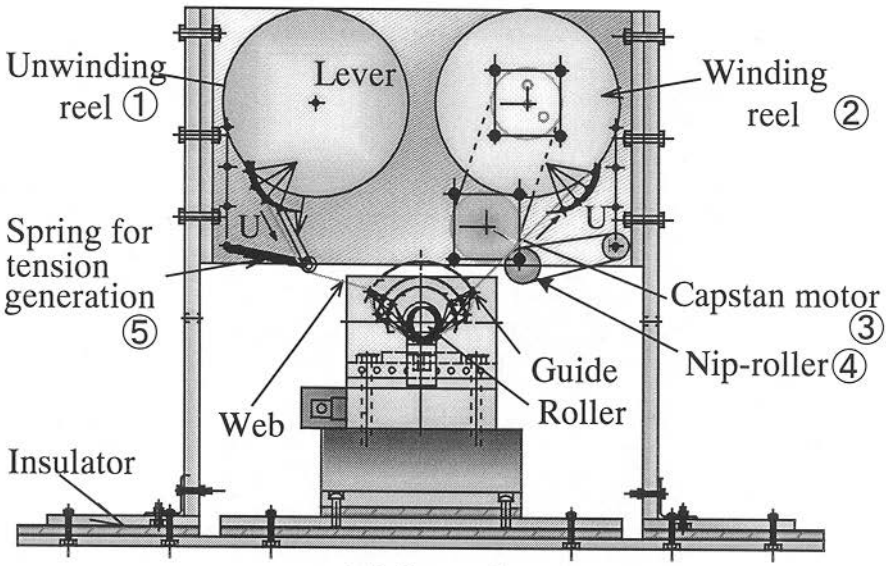

(a) Overview

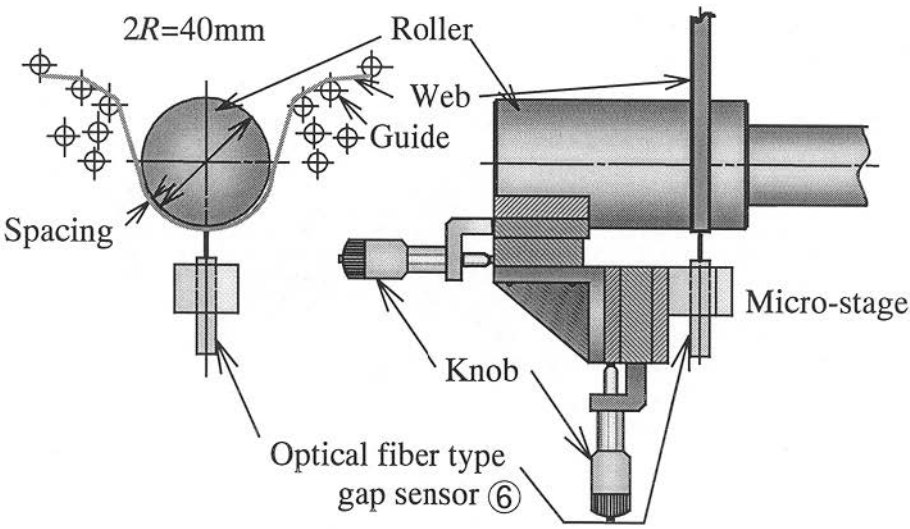

(b) Details in measuring part

Fig. 8 Experimental apparatus

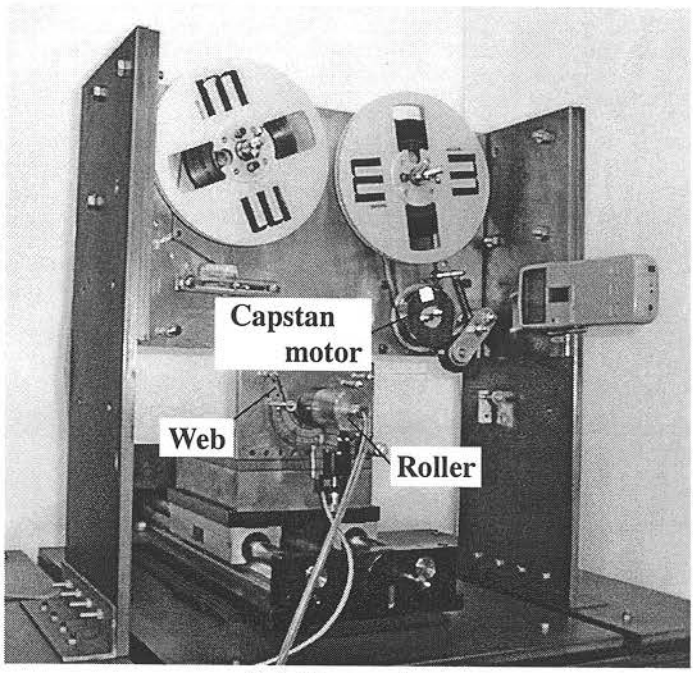

(a) Overview

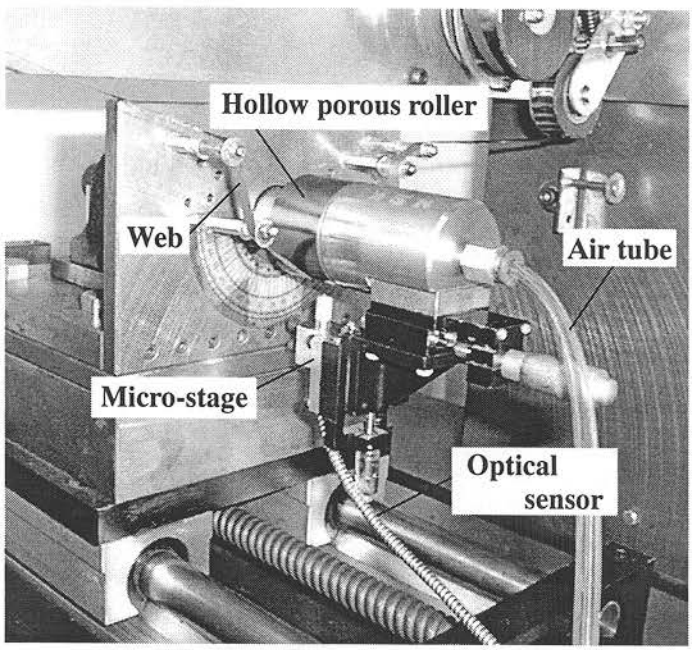

(b) Porous roller and optical sensor

Fig.9 Experimental apparatus

Table 1 Dimensions of flat roller

Radius of roller	$R = 2 \times 10^{-2}$	(m)
Width of web	$L = 6.0 \times 10^{-3}$	(m)
Wrap angle of web	$2B = 66$	(deg)

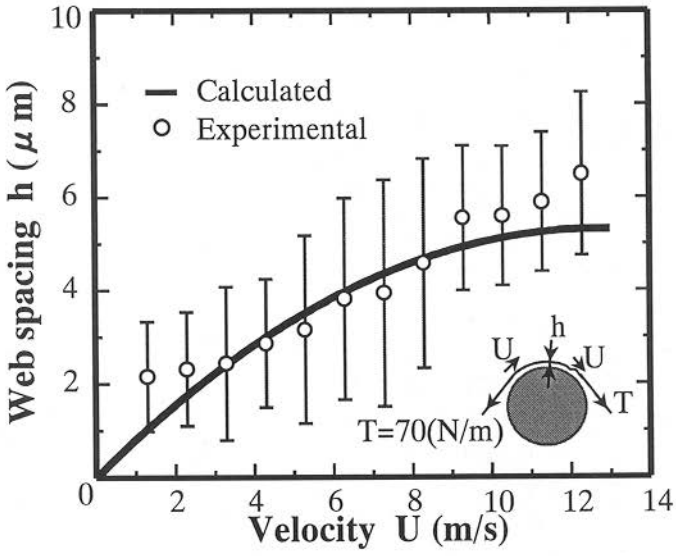

Fig.10 Variation of web spacing with web traveling velocity for flat roller

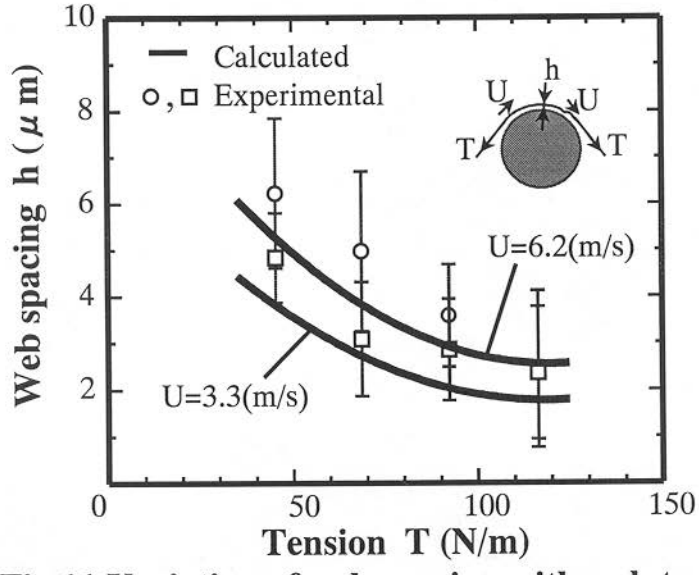

Fig.11 Variation of web spacing with web tension for flat roller

Table 2 Dimensions of hollow porous roller

Radius of roller	$R = 2 \times 10^{-2}$	(m)
Thickness of hollow porous roller	$t = 7.5 \times 10^{-3}$	(m)
Permeability of hollow porous roller	$k = 1.0 \times 10^{-11}$	(m^2)
Width of web	$L = 6.0 \times 10^{-3}$	(m)
Thickness of web	$t_f = 2.3 \times 10^{-5}$	(m)
Wrap angle of web	$2B = 66$	(deg)

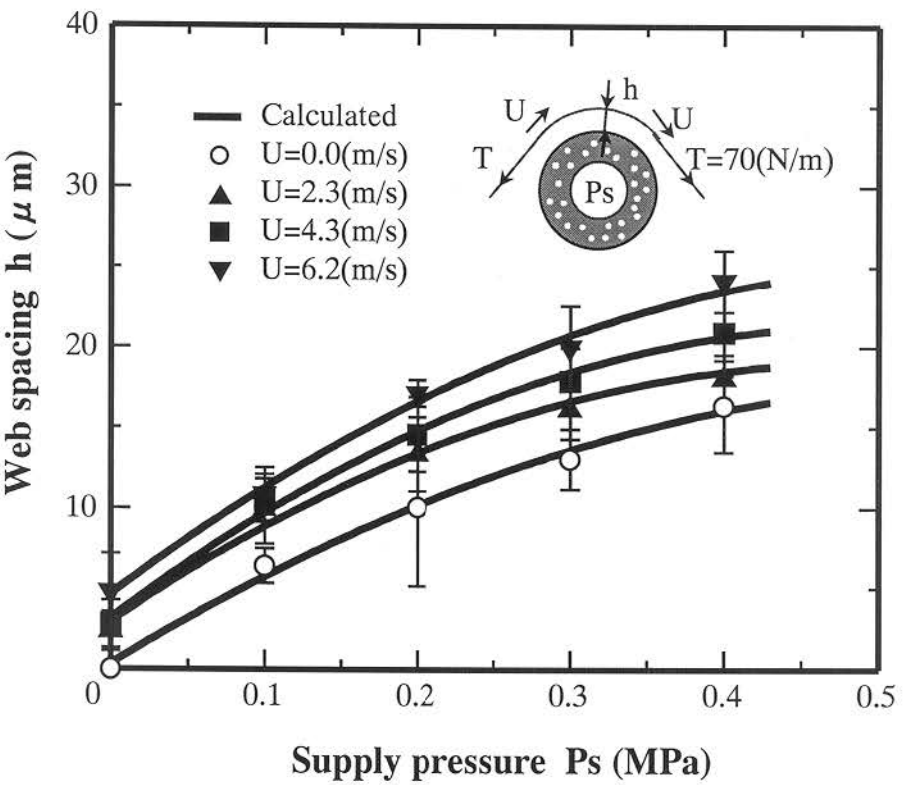

Fig.12 Variation of web spacing with supply pressure for hollow porous roller

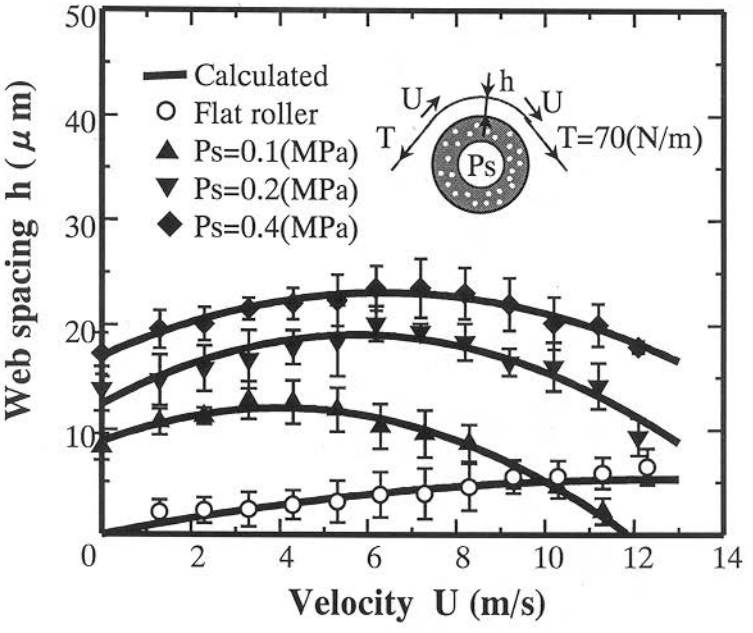

Fig.13 Variation of web spacing with web moving velocity for hollow porous roller

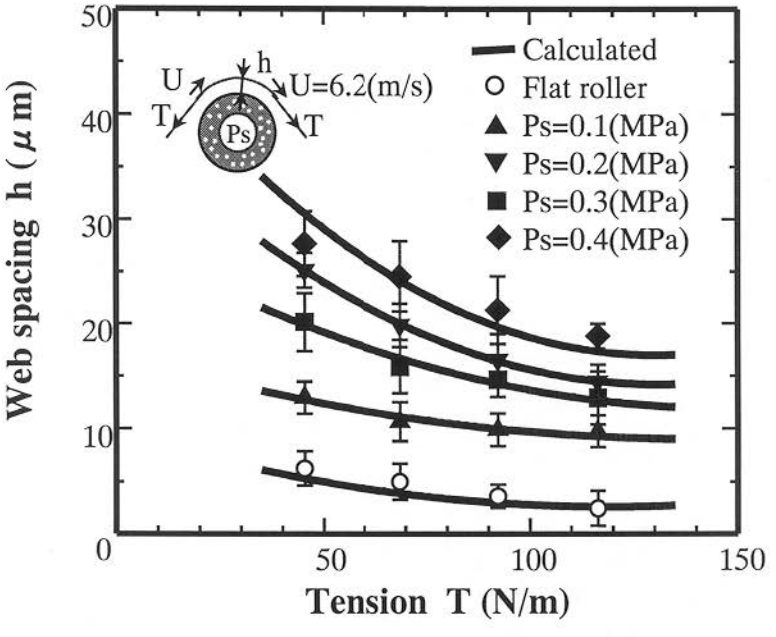

Fig.14 Variation of web spacing with web tension for hollow porous roller

Table 3 Dimensions of rectangular grooved roller

Radius of roller	$R = 2 \times 10^{-2}$ (m)
Groove width	$b_g = 1.0 \times 10^{-4}$ (m)
Groove depth	$h_g = 1.0 \times 10^{-4}$ (m)
Groove pitch	$b = 2.5 \times 10^{-3}$ (m)
Width of web	$L = 6.0 \times 10^{-3}$ (m)
Thickness of web	$t_f = 2.3 \times 10^{-5}$ (m)
Wrap angle of web	$2B = 66$ (deg)

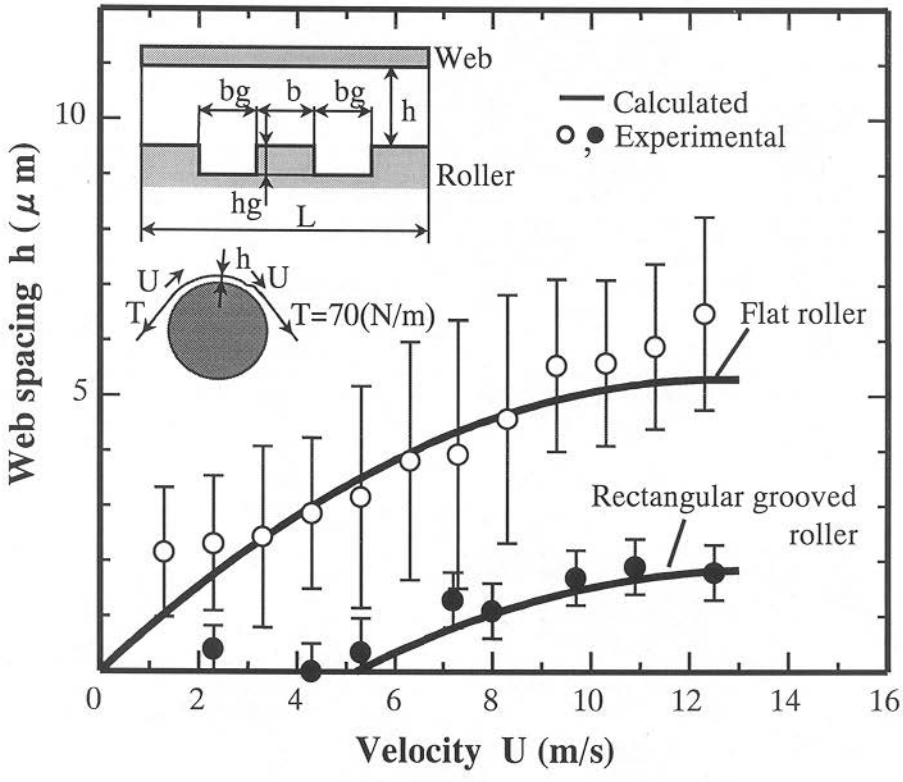

Fig.15 Variation of web spacing with moving velocity for rectangular grooved roller

Table 4 Dimensions of triangular grooved roller

Radius of roller	$R = 2 \times 10^{-2}$ (m)
Groove width	$b_g = 2.0 \times 10^{-4}$ (m)
Groove depth	$h_g = 1.0 \times 10^{-4}$ (m)
Groove pitch	$b = 2.5 \times 10^{-3}$ (m)
Width of web	$L = 6.0 \times 10^{-3}$ (m)
Thickness of web	$t_f = 2.3 \times 10^{-5}$ (m)
Wrap angle of web	$2B = 66$ (deg)

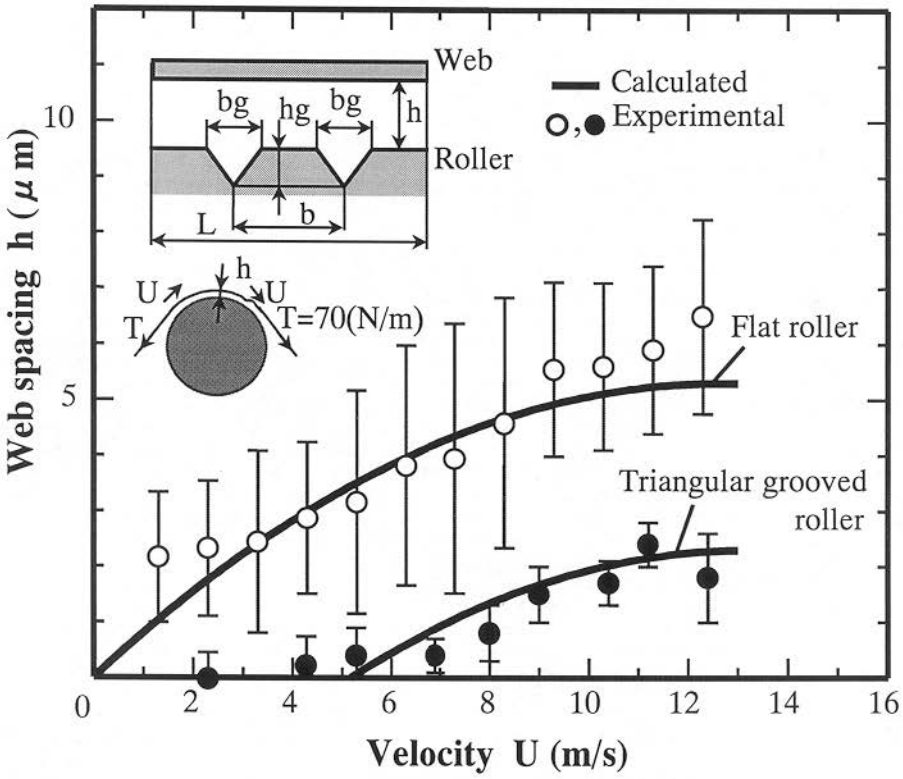

Fig.16 Variation of web spacing with moving velocity for triangular grooved roller

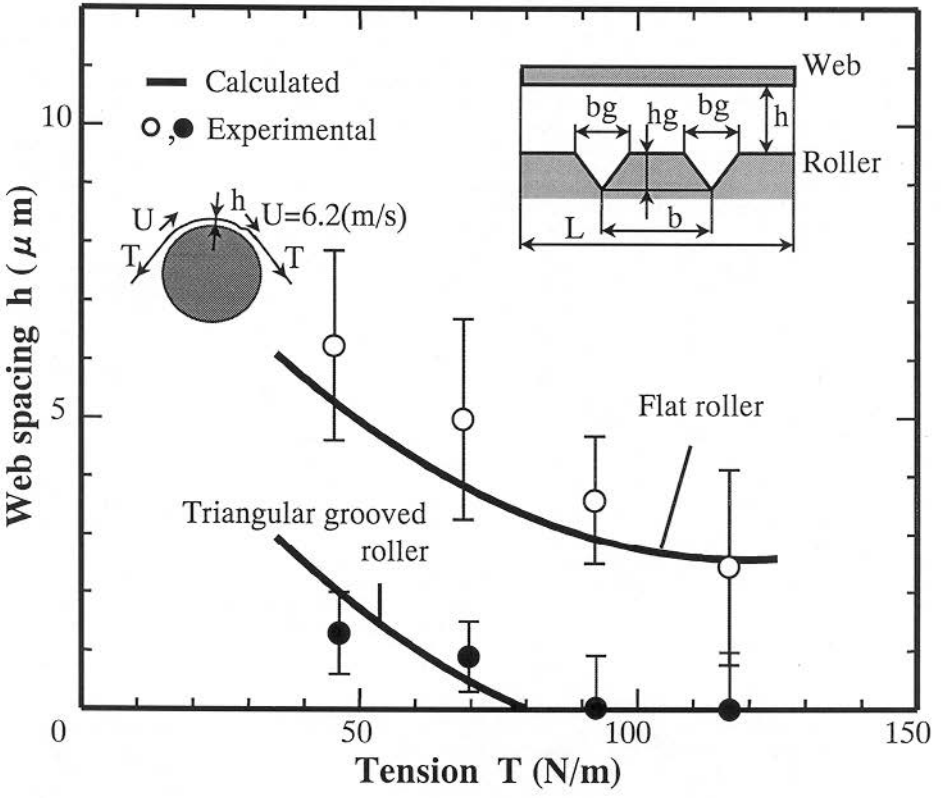

Fig.17 Variation of web spacing with tension for triangular grooved roller

H. Hashimoto
Improvement of Web Spacing Characteristics by Two Types of Guide Rollers
6/9/99 Session 4 1:25 - 1:50 p.m.

Question - David Pfeiffer, JDP Innovations
Sweeny and Nox would have predicted a minimum of gap clearance under velocity of a moving web about 60% of the way around the wrap. Did you find a minimum spacing point at 60% way around or so?

Answer – H. Hashimoto, Tokai University
In my oscillation, you might just find the minimum point near outlet of web wrapped region, and the ratio of minimum film thickness to the constant film thickness is about 0.8, it is independent of the wrap angle and the web width.

Questions - Y. B. Chang, Oklahoma State University
One slide showed that the air gap increases a little with the moving speed and then decreases again. Can you explain a little more how the air gap can be reduced with the speed of the web.

Answer - H. Hashimoto, Tokai University
I also want to know why! In both calculated and measured results, we found the same phenomena. The higher hydrodynamic air pressure may be predominant as compared with hydro static pressure if the web moving speed becomes higher and higher, maybe the inverse flow will induced from the gap to the inside of the roller. I would like to verify the phenomena by applying the visualization technique in the near future. This is important question for me.

Questions:
How did you measure the porosity of your roller; I see you have units of meter squared. Is there some kind of time unit in you porosity units? How many holes per meters square?

Answer - H. Hashimoto, Tokai University
I didn't measure it. It depends on the company measurement, I used a fixed value of permeability of the roller which was made by the company.